Applied Catalysis A: General 475 (2014) 226–234

Contents lists available at ScienceDirect

Applied Catalysis A: General

journal homepage: www.elsevier.com/locate/apcata

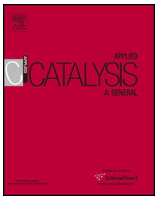

Cellulose hydrolysis over silica modified with chlorosulphonic acid in one pot synthesis

Kasim Mohammed Hello[a,*], Hathama Rzooki Hasan[b], Muna Hasoon Sauodi[b], Per Morgen[c]

[a] Chemistry Department, College of Science, Al-Muthanna University, Al-Samawa, Iraq
[b] Chemistry Department, College of Science, University of Baghdad, Baghdad, Iraq
[c] Department of Physics, Chemistry and Pharmacy, University of Southern Denmark, Campusvej 55, Odense M, Denmark

ARTICLE INFO

Article history:
Received 4 October 2013
Received in revised form 13 January 2014
Accepted 16 January 2014
Available online 24 January 2014

Keywords:
Surface modification
Cellulose
Rice husk ash
Chlorosulphonic acid
Glucose

ABSTRACT

Titration of chlorosulphonic acid against sodium silicate was carried out via a simple one pot synthesis at room temperature to form an acid catalyst denoted as $RHSO_3H$. The BET measurements of the catalyst showed the surface area to be 80 $m^2 g^{-1}$. The FT-IR clearly showed the presence of $-SO_2-$ absorption band at the expected range. The XPS showed the presence of O, Si, and S. The presence of S 2p on the XPS spectra indicated that the sulphonic acid groups ($-SO_3H$) are included into the catalyst structure. The $RHSO_3H$ was efficient for the hydrolysis of cellulose, with maximum glucose yields over 99% at 120 °C with 100% selectivity. As the solubility of cellulose is very important factor to make the hydrolysis much more easily. It was observed that the mixture of DMF/LiCl or cyclohexanol/LiCl has high ability to dissolve cellulose. The catalyst was simple in its preparation, stable during the cellulose hydrolysis in addition to repeatedly without a significant loss of its catalytic activity.

1. Introduction

Over the last two decades, a special attention has been paid to the rice husk (RH). Due to it being available free, with a high silica content and suitable for recycling makes it economically viable to be used as a raw material [1]. The controlled burning of RH in air leads to the formation of rice husk ash (RHA), which contains ca. 95% silica [2]. RHA is a great environment threat causing damage to land and surrounding area where it is dumped. Therefore, commercial use of RH and its ash is the alternative solution to disposal problem.

Nowadays the environmental benefits of wood or other forms of biomass/agricultural wastes associated with the producing of solid, liquid and gaseous fuels which is attracting wide attention. Agricultural waste has an important contributor into the world economy. Today, various forms of agricultural wastes energy are consumed all over the world [3]. Cellulose is a bioorganic molecule with a long linear chain polymer of several monomeric D-glucose units linked by β-1,4-glycosidic bonds. It is the most abundant organic compound in nature and does exist in the cell wall of plants as complex fibrous carbohydrates [4]. Natural fibers mainly consist of cellulose, lignin, and hemicellulose in addition to low quantities of pectin, pigments and extracts.

Cellulose hydrolysis can be achieved by using enzymes [5], or by diluting and concentrating acids [6]. In a preliminary experiment, cellulose was hydrolyzed using 70% w/w sulphuric acid in a sealed reactor. After 9 h of hydrolysis, there was approximately 31% of the glucose has been obtained [7]. A new route to high yield sugars from cellulose based upon the use of phosphoric acid 60% and sulphuric acid 70% at 85 °C for hydrolysis, this route produced glucose with a yield of approximately 90% after about 4 h of hydrolysis [8]. While Changzhi et al. [9] hydrolyzed cellulose at 175 °C for 7 h using 85% H_3PO_4 as a catalyst, there is only16% of the glucose was obtained under these conditions.

In the present study, the modification of silica extracted from RH with chlorosulphonic acid was described in more direct and simple method. As the product is a solid acid, it can be applied in the hydrolysis of cellulose to glucose.

2. Materials and method

2.1. Raw materials

The chemicals used in this study were Sodium hydroxide (Systerm, 99%), Aceton (GCC, 99%), Nitric acid (Scharlau, 65%), 1-Butanol (Fluka, 99%), Cellulose (Riedle-De Haen 99%), Chlorosulphonic acid

---

* Corresponding author. Tel.: +964 7801274886.
E-mail addresses: kasimhello@gmail.com, kasimaz@yahoo.com (K.M. Hello).

http://dx.doi.org/10.1016/j.apcata.2014.01.035
0926-860X/© 2014 Elsevier B.V. All rights reserved.

(J.T. Baker, 99.8%), Cyclohexanol (Riedle-De Haen, 99%), Dimethylformamide (DMF) (Systerm, 99.5%), Dinitrosalycilic acid (DNS) (BDH, 99%), Dioxane (Riedel-De Haen, 99.5%), Glucose (BDH, 99%), Lithum chloride (Sigma, 99%), Sulphuric acid (Poch, 95%), Toluene (GCC, 95%). The RH was collected from a rice mill in Samawah, Iraq. All other chemicals used were AR grade or of high purity and were used directly without further purification.

2.2. Extraction and modification of silica from RHA

2.2.1. Sources of silica

The RH was chosen as the source of amorphous silica [10] as it was available in abundance. The silica was extracted from RH according to a reported method [11,12].

2.2.2. The one-step preparation of solid silica-sulphonic acid

About 3.0 g of RHA was added to 100 mL of 1.0 M NaOH in a plastic container and stirred for 30 min at room temperature to converted silica to sodium silicate. The sodium silicate formed was filtered to remove undissolved particles. The solution was then titrated slowly with 3.0 M nitric acid and 3.0 mL (51.0 mmol) of chlorosulphonic acid with constant stirring. The change in pH was monitored by using a pH meter. A white gel started to form when the pH reached 10.0. The titration was continued until the pH of the solution reached 3.0. The gel was aged for 24 h at room temperature. It was later separated by centrifuge. The separation process was repeated 6 times with copious amount of distilled water, and the final washing was done with acetone. The sample was then dried at 110 °C for 24 h and finally, it was ground to a fine powder, which weighed 6.4 g. It was labelled as $RHSO_3H$.

2.3. Sample characterization

The $RHSO_3H$ was characterized by Powder X-ray diffraction (Systerm). XPS was performed in a SPECS system, including a Phoibos 100 analyzer. The samples were in the form of a white small size grained powder. This powder was deposited on the top surface of a double sided sticky carbon tape attached to a stainless steel sample holder. The deposited powder was uniformly covering the carbon tape and inserted in the vacuum system and pumped down to 3×10^{-10} Torr overnight. XPS spectra were recorded with Mg K_{alpha} and Al K_{alpha} radiation, and the spectra were compared to discriminate between Auger and photoemission peaks. Two spectra are shown: A wide scan spectrum covering a wide range of binding (and kinetic-) energies, recorded with Al K_{alpha} radiation, and a resolution of around 2.5 eV, for monitoring the concentration of the elements in the sample, and a detailed scan with a resolution of 1.4 eV, which serves to detect chemical shifts and to separate overlapping peaks. The latter spectrum was recorded with Mg K_{alpha} radiation, which gives a slightly better resolution than for Al K_{alpha}. The resolution for the survey scans was 2.5 eV. Element peaks were identified with the CasaXPS software. The FT-IR spectra were recorded on a 8400 S Shimadzu using KBr disk. UV–visible was recorded on a I65o pc Shimadzu. The scanning electron microscopy (SEM) was recorded on a (Leica Cambridge S360) and energy dispersive spectrometry (EDX) (Edax Falcon System). The Atomic Force Microscopy (AFM) were obtained using CSPM-AA3000, SEM/EDX (Leo 35VP from Zeiss) AEM (PHI Model 560).

2.3.1. Cation exchange capacity (CEC)

1.0 g of sodium chloride was dissolved in 25 mL of distilled water in a conical flask with a magnetic stirrer. 1.0 g (±10 mg) sample of $RHSO_3H$ was added to the solution and left to stir for 30 min. 2–3 drops of phenolphthalein was added and the sample was titrated with standard NaOH solution. An average of three separate titrations was performed to obtain an average value for the CEC of $RHSO_3H$.

2.3.2. Pyridine acidity test

The sample, together with a beaker containing pyridine was placed in a dessicator equipped with a valve connected to a membrane vacuum pump (AMB Greiffenberger Antriebstechnik, MZ2C, CE 2002/06). The system was evacuated for 1 h at a rate of $1.7\ m^3\ h^{-1}$. The system was kept under closed vacuum for 48 h. The atmosphere in the desicator was evacuated again for 1 h at the same pump rate. The sample was then removed and analyzed by FT-IR in KBr disc.

2.4. Catalytic hydrolysis procedure

2.4.1. Hydrolysis of cellulose

The cellulose hydrolysis was carried out in liquid-phase in a 50 mL round bottom flask equipped with magnetic stirrer and water condenser. 20 mL of DMF, 0.2 g of LiCl and cellulose (0.18 g, 20 mmol) were separately transferred to the round bottom flask containing 0.2 g of the catalyst (pre-dried at 110 °C for 24 h and cooled in desiccators to minimize moisture content). The hydrolysis temperature fixed at 120 °C. The hydrolysis mixture was refluxed for 8 h. A 0.5 mL portion of the clear hydrolyte solution from the reaction mixture was transferred into a vial and 2.0 mL of deionized water was added. To this solution 2.0 mL of DNS reagent and 2.0 mL of 2.0 N NaOH were added and the mixture was incubated in a water bath maintained at 90 °C for 5 min [13,14]. The DNS reagent was prepared according to an IUPAC method [15]. The reagent blank sample was prepared with 2.0 mL of deionized water, 2.0 mL of DNS reagent and 2.0 mL of 2.0 N NaOH and heated similar to the samples. Then the absorbance was measured at 540 nm, against the reagent blank, and glucose concentrations in solutions were calculated by employing a standard curve prepared using glucose. The catalytic activity with different mass of catalyst (50, 100, 150, and 200 mg), different temperatures (RT, 100, 110, and 120 °C), different solvents i.e. (toluene, dioxane, 1-butanol, cyclohexanol, and ethanol), and RHA-blank catalyst were studied by using the same procedure as in above.

2.4.2. The reusability of the catalyst

Reusability experiment was conducted by running the hydrolysis successively with the same catalyst under the same hydrolysis condition. The hydrolysis was first run with the fresh catalyst to complete conversion and then the catalyst was filtered and washed with hot dioxane then with hot mixture of DMF and LiCl and dried at 110 °C. After regeneration, the catalysts were reused under the optimised reaction conditions.

2.4.3. Hydrolysis procedure for homogenous catalyst

The hydrolysis using homogenous catalyst was studied with sulphuric acid. Typically, a 50 mL capacity two necked round-bottom flask, equipped with a magnetic stirrer (700 rpm) and water condenser was used. 20 mL of DMF was transferred by pipette into the round bottom flask containing 8.8 mg (6.9 mmol) of sulphuric acid. After the reaction temperature reached 120 °C, 0.18 g (20.0 mmol) of cellulose was added. The hydrolysis mixture was refluxed. Samples for analysis (~0.50 mL) were withdrawn at regular intervals from the hydrolysis mixture by means of a syringe equipped with filter (cotton wool). To this solution 2.0 mL of DNS reagent and 2.0 mL of 2.0 N NaOH were added and the mixture was incubated in a water bath maintained at 90 °C for 5 min. The glucose concentrations in solutions were calculated by employing a standard curve prepared using glucose.

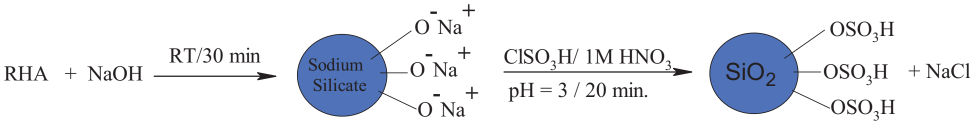

Scheme 1. The reaction sequence for the direct synthesis of $RHSO_3H$. The approximate time taken for the completion of the experimental process was less than 60 min.

3. Results and discussion

3.1. The synthesis

Silica which extracted from RHA has been modified with chlorosulphonic acid in one pot synthesis at room temperature and pressure. Scheme 1 shows the synthesis of $RHSO_3H$. The RHA has been characterized elsewhere [16].

3.2. Powder X-ray diffraction (XRD)

Fig. 1(a and b) shows XRD pattern of RHA and $RHSO_3H$. A broad diffraction band at 2θ angle of ca. 22° in Fig. 1(a and b) was observed. This was typically referred to amorphous silica. This similar to the observation was cited by Adam et al. [17] and Yalçin, et al. [18]. According the JCPDS files in Fig. 1(b), the patterns at 2θ angle of ca. 28°, 33° were due to the formation of NaCl. While the patterns at 2θ angle of ca. 29°, 34°, 38°, 48° were due to the formation of Na_2SiO_3. This result was supported by XPS result as will explain latter. Both NaCl and Na_2SiO_3 were come from the synthesis of the catalyst. This result is in agreement well with the literature [19]. The patterns at 2θ angle of ca. 14°, 19° were due to the presence of sulphur onto silica surface [20]. The presence of sulphur may indicate that the sulphonic acid was immobilized onto silica.

3.3. The nitrogen adsorption analysis

Fig. 2 shows the nitrogen adsorption isotherm obtained for $RHSO_3H$ and inset is shown the pore size distribution graph. The hysteresis loop observed in the range of $0.4 < P/Po < 1.0$, is associated with capillary condensation according to IUPAC classification. The isotherm shown is of type IV and exhibited an H3 hystereis loop [21].

The BET analysis showed the specific surface area of $RHSO_3H$ was 80 $m^2\,g^{-1}$, while the specific surface area of RHA which was reported to be 347 $m^2\,g^{-1}$ [16]. The decrease in the surface area of

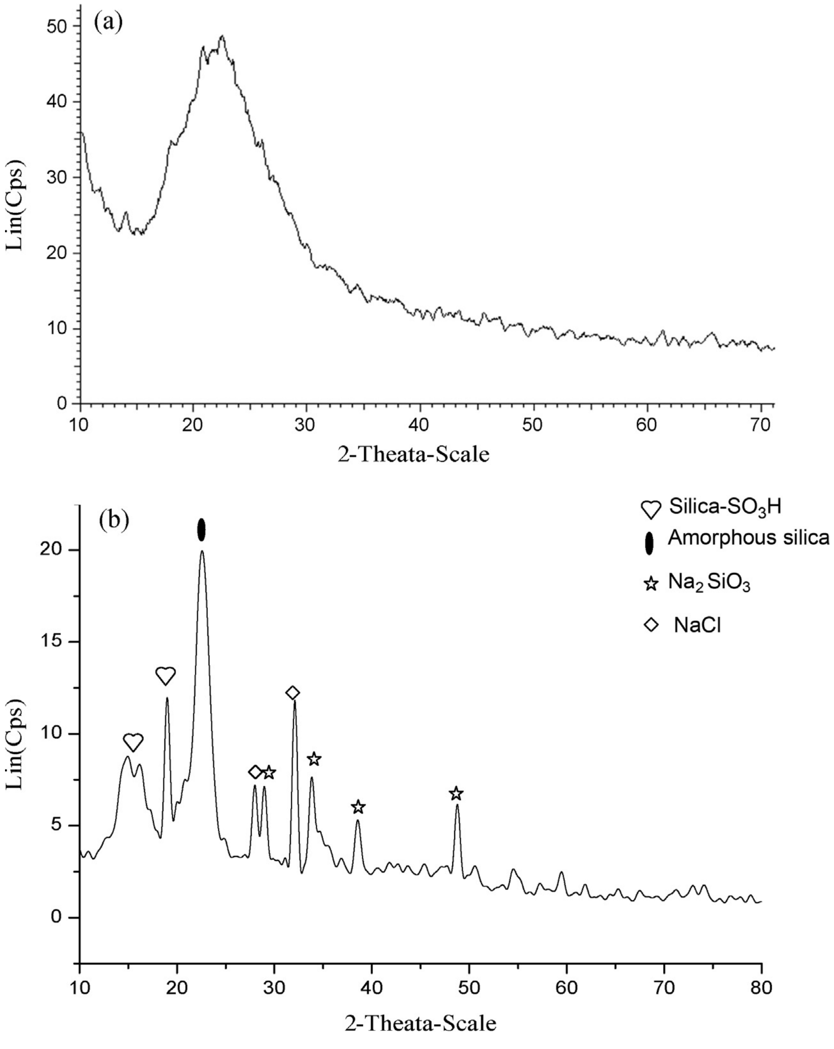

Fig. 1. The X-ray diffraction pattern for RHA and $RHSO_3H$. (a) XRD of RHA, (b) XRD of $RHSO_3H$.

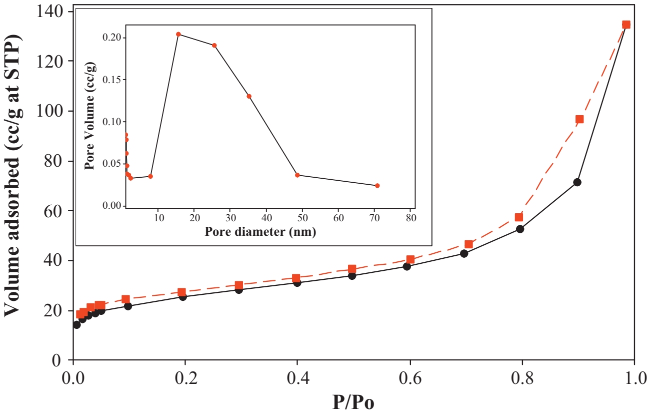

Fig. 2. The N_2 adsorption/desorption isotherms of $RHSO_3H$ with the corresponding pore size distribution inset.

$RHSO_3H$, however, could be due to the reduction of the surface sites by chlorosulphonic acid causing the surface to be over crowded with the ligand network on the surface and thus blocked the pores. The $RHSO_3H$ (Fig. 2) showed a broad pore size range from 10 to 50 nm which is in the mesoporous range.

3.4. *Fourier transformed infrared spectroscopy analysis (FT-IR)*

Fig. 3 shows the FT-IR spectra of RHA and $RHSO_3H$ spectrum. The strong and broad band in the range of 3500–3455 cm^{-1} region corresponds to the hydrogen bonded from SiO–H and HO–H of adsorbed water. The band at 1639 cm^{-1} is due to the HO–H of adsorbed water. The $RHSO_3H$ spectrum shows bands at 1384–1201 cm^{-1} is due to the asymmetric and symmetric stretching bands of $-SO_2-$ moieties, which confirm the formation of sulphonic acid [22]. The RHA spectrum does not show these bands. In RHA the Si–O–Si vibration appears at 1099 cm^{-1} [11]. This vibration was observed displaced to 1051 cm^{-1} in $RHSO_3H$. This reflects the chemical transformation that is taking place adjacent to the –Si–O–Si– framework by chlorosulphonic acid.

3.5. *X-ray photoelectron spectra (XPS)*

The photoelectron peaks of O 1s, Si 2p, S 2p of the catalyst are presented in Fig. 4(a and b). The formation of sulphur–oxygen species, which typically have binding energy in region 167–169 eV, is already seen. Spectral peak of S 2p XPS of $RHSO_3H$ has been occurred at ca. 168–169 eV associated with sulphate (S 6+) species due to sulphonic acid groups ($-SO_3H$). This result was consistent with a previous study [23]. The O 1s binding energy was found at 532.3 eV for $RHSO_3H$ while the Si 2p binding energy at 102.7 eV that was obtained from an overlap of Si 2p3/2 and Si 2p1/2 binding energy [24]. The XPS has also shown a peak at ca. 1070 eV associated with Na 1s species, the presence of Na due to synthesis process of the catalyst. In order to better observation of sulphonic groups, the XPS spectrum between 250 and 0 eV was included (Fig. 4b). The positions of all the peaks in the spectra have been shifted (around 5 eV) to compensate for charging of the sample due to the X-ray beam, and a low conductivity of the powder sample. With this shift the O 1s line is brought to a position of a 532 eV binding energy. The S and Si peaks are shifted about 4 eV with respect to their neutral positions, after this alignment of the spectrum for the O 1s peak position. This indicates that all Si and S present in the sample are oxidized. The XPS results imply that the chlorosulphonic acid was immobilized onto silica.

3.6. *Scanning electron microscope (SEM)*

The SEM of $RHSO_3H$ was shown in Fig. 5. It seems that the catalyst has shown some rocky particles appear on the surface. It is also indicated that the surface was highly rough and porous.

3.7. *Atomic force microscopy imaging (AFM)*

The AFM images technique was used to characterize topographical and morphological on the $RHSO_3H$ surfaces. Sup. 1(a, b and c)

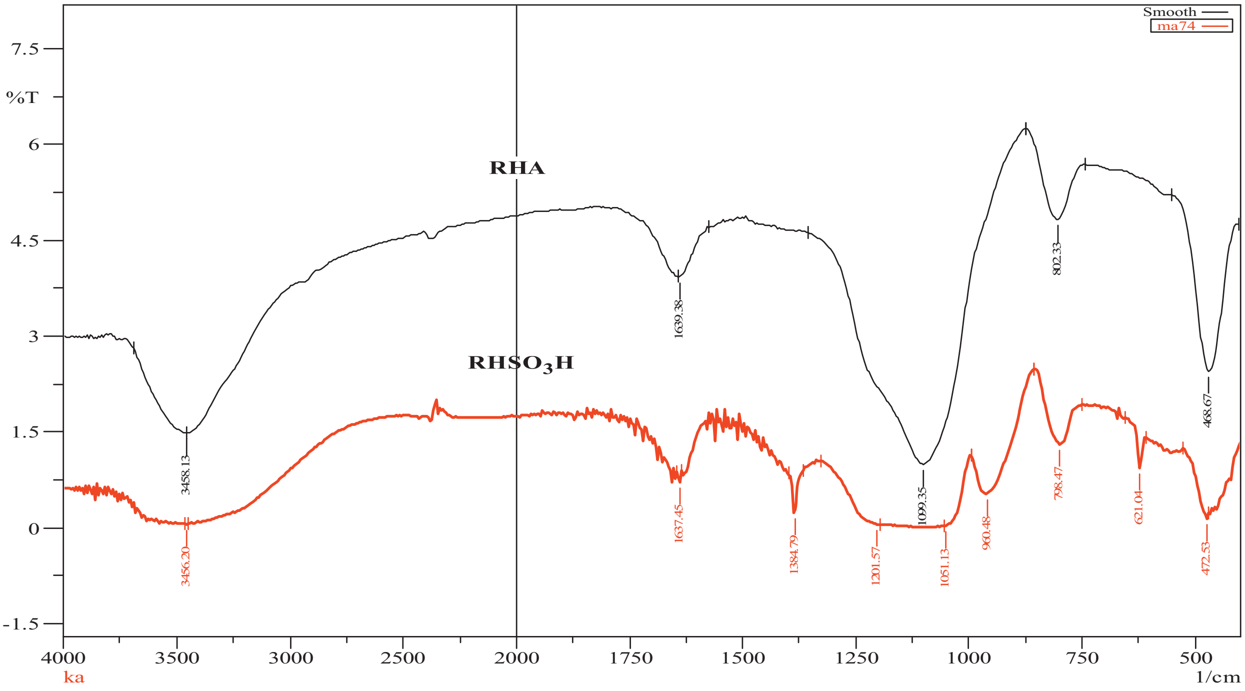

Fig. 3. The FT-IR of RHA and $RHSO_3H$.

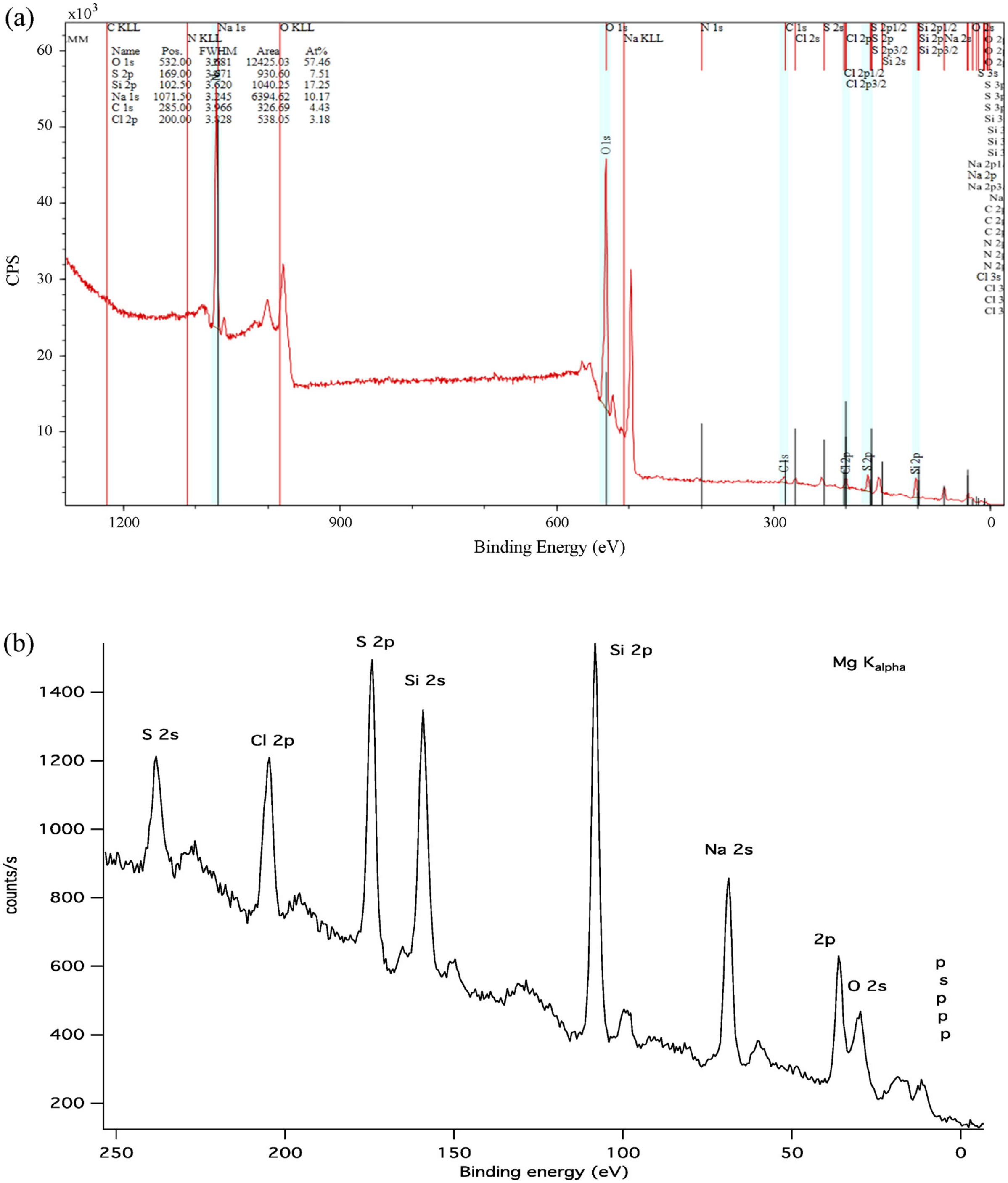

Name	Pos.	FWHM	Area	At%
O 1s	532.00	3.681	12425.03	57.46
S 2p	169.00	3.671	930.60	7.51
Si 2p	102.50	3.620	1040.25	17.25
Na 1s	1071.50	3.245	6394.62	10.17
C 1s	285.00	3.966	326.69	4.43
Cl 2p	200.00	3.328	538.05	3.18

Fig. 4. The XPS spectrum of $RHSO_3H$. The Si, S and O content are shown. (a) A wide scan spectrum, (b) the XPS spectrum between 250 and 0 eV.

shows the AFM of $RHSO_3H$ a relative layer surface with a mean value of surface roughness (Rq) 1.09 nm. The granularity accumulation distribution chart Sup. 1(c) shows the distribution of the particle size. It was observed that the particles were distributed in the range of 70–160 nm. This indicates that the most of the catalyst particles were in nano size.

3.8. *Pyridine test*

The easiest and direct method to distinguish between Brönsted and Lewis acid species is the IR spectroscopy of chemisorbed pyridine. Sup. 2 shows the $RHSO_3H$ after and before pyridine acidity test in absorbance mode using KBr disc at the range of 1700–1400 cm^{-1}. The FT-IR shows bands of the pyridinium ion can be distinguished at 1633 and 1547 cm^{-1} which corresponding to the Brönsted acid species. The band at 1433 cm^{-1} corresponding to hydrogen bonded pyridine [25]. The band at 1494 cm^{-1} [26] was due to the interaction of silanol with Pyridine. These bands did not show up in the spectra before the Pyridine test.

3.9. *Cation exchange capacity (CEC)*

The base titration is generally regarded as a technique that can reasonably be used to calculate the concentrations of acid sites of

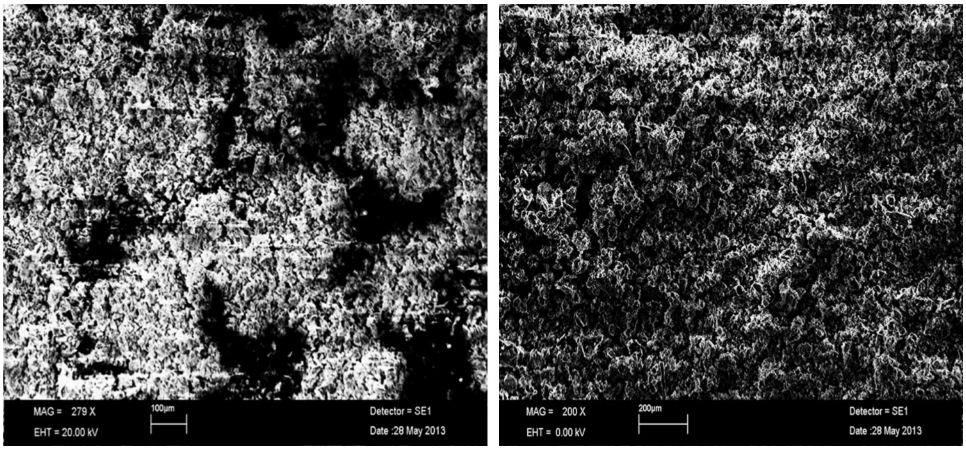

Fig. 5. The SEM micrographs of $RHSO_3H$ at different magnification.

related solid acids. In this work, NaOH as the basic probe compound was used [27]. The CEC was determined by using the following formula [28].

$$\mathrm{CEC} = \frac{\text{Normality of NaOH} \times \text{Volume of NaOH}}{\text{g of material}}$$

The concentrations of acid sites on the $RHSO_3H$ was determined in water, by exchanging with excess Na^+ (from NaCl) followed by titration with a standard NaOH solution. The CEC was found to be 0.07 mequiv/g. However, the low CEC value can be attributed to the poor accessibility of the sulphonic acid group by the titrating base [29]. Some authors cited that the low CEC results associated with sulphonic acid groups buried deep within the silica frame work [30,31]. Another possible explanation is the crowdedness of sulphonic groups in the pore walls of the catalyst thereby limiting the exchange capacity between NaCl and the sulphonic acid group before the titration [32].

3.10. Hydrolysis of cellulose over $RHSO_3H$ catalyst

The $RHSO_3H$ was used to hydrolyze cellulose in liquid-phase reaction using new solvent system. Further various parameters such as effect of hydrolysis time, mass of catalyst, temperature, solvents effects on glucose formation were evaluated to optimize the hydrolysis conditions.

3.10.1. Influence of hydrolysis time

The effect of the hydrolysis time on the hydrolysis of cellulose over $RHSO_3H$, RHA-Blank as well as homogenous sulphuric acid and the new solvent system without catalyst (DMF/LiCl) are shown in Fig. 6. The hydrolysis was carried out with 200 mg catalyst using a DMF/LiCl as a solvent at 120 °C. The initial hydrolysis of cellulose during the first hour was 2% and it reached the maximum hydrolysis 99% in 8 h. The homogeneous sulphuric acid (8.8 mg, 6.9 mmol) showed 80% at 4 h and then the hydrolysis was decreased due to the hydrolysis of glucose itself. It was well known that the homogenous catalyst is more effective than the heterogeneous one. The hydrolysis of cellulose over H_2SO_4 was reached to the optimum at the 4 h of the hydrolysis time then it decrease due to the hydrolysis of the glucose to another products. The hydrolysis of cellulose over $RHSO_3H$ was reached to the optimum at the 8 h of the hydrolysis time. At this point the behaviour of both catalysts is same the only difference is time. At the optimum time of the cellulose hydrolysis over $RHSO_3H$, we did not deduct any hydrolysis of glucose. After the optimum time of the cellulose hydrolysis over $RHSO_3H$, the glucose was started to hydrolyze to other products too. Such a work is under process on our laboratory. The selectivity of the hydrolysis of cellulose to glucose was 100% at the optimum time of the hydrolysis. In our previous studies, we had been immobilized different silica-SO_3H acid catalysts for different purposes [1,2,29,33]. Even these catalysts had low acid density; they had shown very good catalytic activities. Therefore, it is saved to conclude that the activity of silica–SO_3H could be due to the strong acid character of the active sulphonated sites. This phenomenon could explain the activity of $RHSO_3H$ which has low CEC and show high activity during the cellulose hydrolysis.

The maximum hydrolysis of cellulose over DMF without catalyst was 14% in 8 h. It was observed that the hydrolysis over RHA-balnk was found to be 20% in 8 h. The activity of RHA could be related to the weak acidity of the silanol group over the surface of silica.

3.10.2. Effect of catalyst mass

The hydrolysis of cellulose was carried out by varying the amount of $RHSO_3H$ between 50 and 200 mg while keeping the other parameter fixed as, 8 h hydrolysis time at 120 °C. The effect of the amount of catalyst on the hydrolysis of cellulose is shown in Fig. 7. When the catalyst mass was increased from 50 to 200 mg, the cellulose hydrolysis increased from 75% to 99%. Further increase of the catalyst mass had no significant effect. The increased in the conversion with the catalyst mass could be attributed to the availability of a greater number of catalytically active sites. Therefore 200 mg was choosing as the optimum mass of the catalyst.

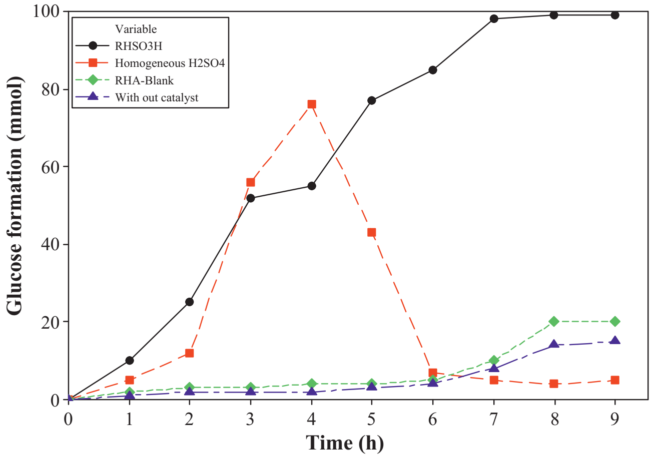

Fig. 6. The hydrolysis of cellulose to glucose over $RHSO_3H$, RHA-blank, sulphuric acid and DMF without catalyst as a function of hydrolysis time. The hydrolysis conditions were: catalyst 200 mg, H_2SO_4 (8.8 mg, 6.9 mmol), and reaction temperature (120 °C).

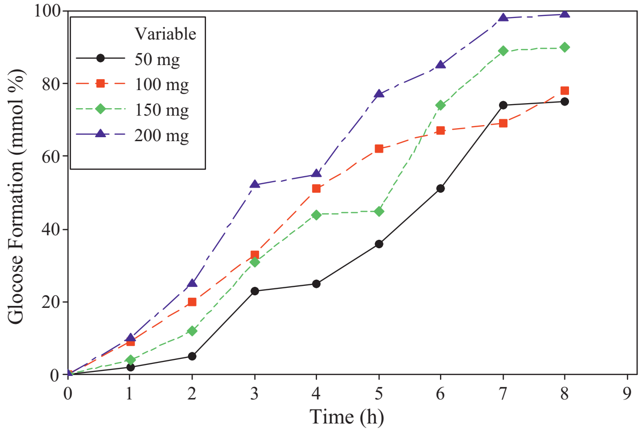

Fig. 7. The hydrolysis of cellulose to glucose over RHSO$_3$H, as a function of mass of catalyst. The hydrolysis conditions were: 8 h hydrolysis time at 120 °C.

3.10.3. Influence of hydrolysis temperature

The effect of temperature on the hydrolysis of cellulose over RHSO$_3$H is shown in Fig. 8. The hydrolysis increased when the reaction temperature was increased from room temperature to 120 °C. The hydrolysis was ca. 99% at 120 °C. Most researchers set the hydrolysis temperature at 100 °C. To confirm the effect of hydrolysis temperature on the yield of glucose, comparing with Xia and co-workers [34] who they have been used different SO$_3$H-functionalized acidic ionic liquids as a homogeneous catalyst for cellulose hydrolysis. The maximum sugar yields at 100 °C were 83% at 2 h. By using RHSO$_3$H the sugar was reach ≈80% at 100 °C and 99% at 120 °C in 8 h. Taken into account the nature of the RHSO$_3$H catalyst used (heterogeneous catalyst) in this study. This clearly indicates that the using of RHSO$_3$H is effective to promote the hydrolysis of cellulose.

3.10.4. Influence of the solvents effect

The hydrolysis of cellulose is varying according to its solubility into different solvents. Cellulose can be dissolved in several complex solvents, such as $Cu(NH_3)_4(OH)_2$, $[NH_2CH_2CH_2NH_2]Cu(OH)_2$, $[NH_2CH_2CH_2NH_2]Zn(OH)_2$, and $([Pd(NH_2(CH_2)_2NH_2)](OH)_2$ [35]. It was mentioned that the cellulose was completely soluble in the N,N-diethylacetamide containing LiCl [36]. Since 1972 up to date lithium chloride/N,N-diethylacetamide has become very popular to dissolve cellulose [37,38]. These early studies showed the uniqueness of LiCl/N,N-diethylacetamide as solvent system.

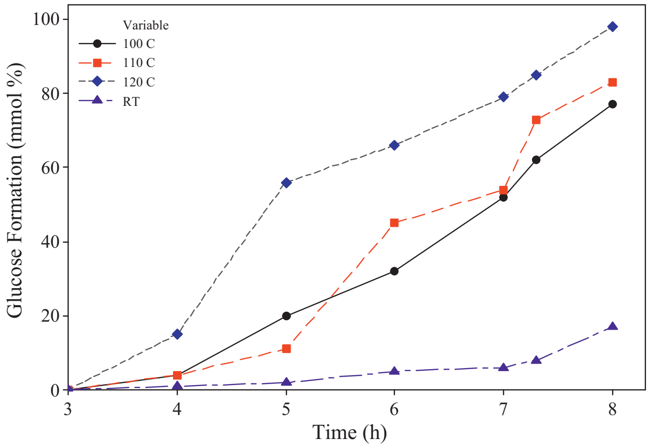

Fig. 8. The hydrolysis of cellulose to glucose over RHSO$_3$H, at different temperatures. The hydrolysis conditions were: catalyst 200 mg, and 8 h reaction time.

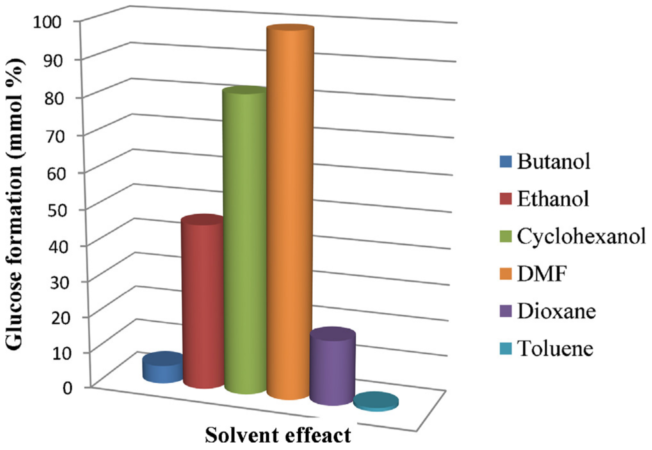

Fig. 9. The hydrolysis of cellulose to glucose over RHSO$_3$H, at different solvents. The hydrolysis conditions were: catalyst 200 mg, 120 °C and 8 h reaction time.

In this study it is found that the cellulose was highly soluble in DMF or cyclohexanol containing LiCl. This phenomenon was not cited before. The solvent–lithium interaction and the chloride ion were playing a vital role in the solubility of cellulose. The lithium ions are tightly linked with the carbonyl group of DMF while the chloride ions are left unencumbered. Thereby Cl^- is highly active as nucleophilic base and plays a major role by breaking up the inter- and intra-hydrogen bonds [39]. This could make the hydrolysis of cellulose much more easily.

The effect of the solvent on the hydrolysis of cellulose over RHSO$_3$H was shown in Fig. 9. The hydrolysis was studied over different solvents i.e. 1-butanol, ethanol, cyclohexanol, dioxane and toluene as well as DMF. All these solvents contain LiCl. It was observed that the hydrolysis of cellulose over these solvents was increased according the following order:

DMF $>$ cyclohexanol $>$ ethanol $>$ dioxane $>$ 1-butanol $>$ toluene

Most of our dissolution system could form hydrogen bonding between layers of cellulose chains and the solvents. The DMF contains more than one centre able to form a hydrogen bonding with the cellulose and this could lead to increasing the solubility of cellulose which makes the hydrolysis easier. The other solvents have only one centre able to form a hydrogen bond with cellulose. While the toluene could not form a hydrogen bond and it has a very low solubility of cellulose.

3.10.5. Catalyst recycles experiments

Fig. 10 shows the RHSO$_3$H recycles experiments. After the first reaction was run using the catalyst at 120 °C for 8 h, the mixture, including the solid catalyst and the cellulose residue, was then filtered and washed with hot dioxane then with hot mixture of DMF and LiCl (repeated three times) and the catalyst was heated at 100 °C for 24 h. Next, fresh cellulose and DMF with LiCl were added to the catalyst obtained and a second run was conducted, as well as a third run, using the same procedure. As shown in Fig. 10, the product yields in the second and third runs were similar to that in the first run, without any loss in the catalytic activity. These results indicated that catalytic performance was not lost in the course of the catalytic runs. Since the evaluation of the catalyst stability is important for practical catalyst use, further studied on the stability of the RHSO$_3$H catalysts in repeated runs was done. The pre-treated RHSO$_3$H catalysts were characterized by FT-IR analysis (see supplementary data, Sup. 3). The FT-IR of the catalysts was not changed after pre-treatment. The analysis data of the textural properties demonstrated that the RHSO$_3$H catalyst had excellent stability during the pre-treatment.

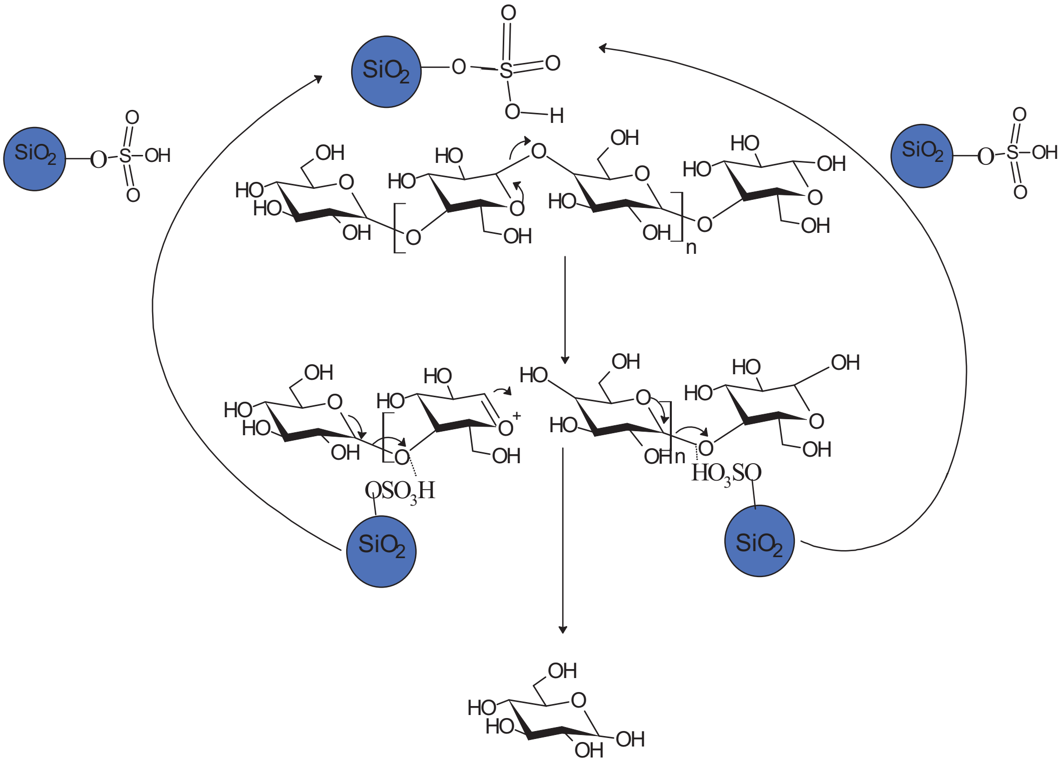

Scheme 2. The possible mechanism of the cellulose hydrolysis to glucose over $RHSO_3H$.

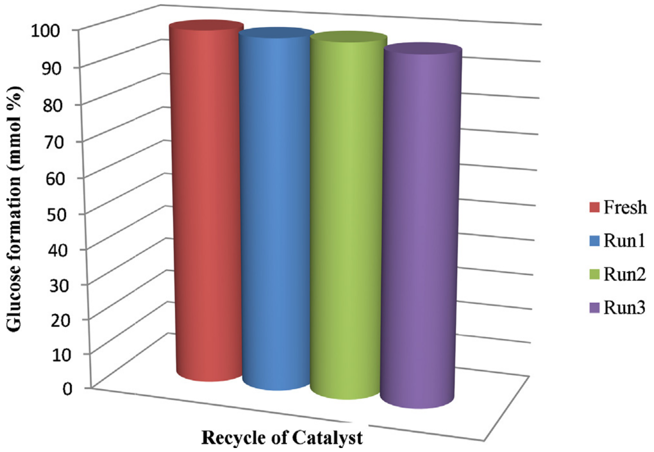

Fig. 10. The hydrolysis of cellulose to glucose over $RHSO_3H$, reusability. The hydrolysis conditions were: catalyst 200 mg, 120 °C and 8 h reaction time.

3.10.6. The mechanism of the hydrolysis of cellulose over $RHSO_3H$

As shown in the characterization techniques which used above, the $RHSO_3H$ has Brönsted acid sites. These acid sites could interact rapidly with the glycosidic oxygen linking two sugar units via a hydrogen bonding between layers of cellulose chains. Then the cleavage of the C–O bond to the cyclic carbonium ion takes place. Finally the yield of monosaccharides after partial hydrolysis is occurred and the catalyst could hydrolyze new cellulose chains as in Scheme 2.

4. Conclusion

Chlorosulphonic acid was reacted with sodium silicate in purely homogenous route to form $RHSO_3H$ with Brönsted acid sites. According to the BET result the $RHSO_3H$ had 80 $m^2\,g^{-1}$ as a specific surface area. The XPS shows the presence of O, Si, S peaks. The presence of S 2p on the XPS spectra indicated that the sulphur has +6 oxidation state which corresponded to the sulphonic acid groups ($-SO_2-$).The FT-IR clearly showed the presence of $-SO_2-$ absorption band at the expected range. The $RHSO_3H$ was used to hydrolyze of cellulose to glucose at 120 °C for 8 h. The catalytic activity of the catalyst reach to 99% of glucose and the selectivity was 100%. It was found that the hydrolysis of cellulose became much more easily when DMF or cyclohexanol containing LiCl were used as a solvent. The catalyst was simple in the preparation, stable during the hydrolysis and could be used several times without significant loss of its catalytic activity.

Acknowledgments

The Authors would like to thank Dr. T. Radika (Scientific Society under M/o Communications and Information Technology, India) for doing some analysis. Special thanks to Dr. Jawad Kadhim (Department of Chemistry, College of Science, Al-Muthanna University) for the critical discussion regarding the manuscript.

References

[1] F. Adam, K.M. Hello, M.R. Ben Aisha, J. Taiwan Inst. Chem. Eng. 42 (2011) 843–851.
[2] F. Adam, K.M. Hello, T.H. Ali, Appl. Catal. A 399 (2011) 42–49.
[3] K. Annamalai, S. Priyadarsan, S. Arumugam, J.M. Sweeten, Energy Eng. Technol. 1 (2007) 476–497.
[4] K.B. Olanrewaju, Reaction kinitics of cellulose hydrolysis in subcritical and supercritical water, PhD. Thesis, University of Iowa, USA, 2012, pp. 7–9.
[5] B. Yu, H.Z. Chen, Bioresour. Technol. 101 (2010) 9114–9119.
[6] S. Wald, C.R. Wilke, H.W. Blanch, Biotechnol. Bioeng. 26 (1984) 221–230.
[7] N. Bhandari, D.G. McDonald, N.N. Bakhshi, Biotechnol. Bioeng. 26 (1984) 320–327.
[8] B.J. Kim, Y.Y. Lee, R. Torget, Appl. Biochem. Biotechnol. 45–46 (1994) 113–129.
[9] Y.Y. Lee, P. Iyer, R.W. Torget, in: G.T. Tsao (Ed.), Dilute-Acid Hydrolysis of Lignocellulosic Biomass, Springer-Verlag, Berlin, 1999, pp. 93–115.
[10] C. Real, M.D. Alcala, J.M. Criado, J. Am. Chem. Soc. 79 (1996) 2012–2016.

[11] F. Adam, J.H. Chua, J. Colloid Interface Sci. 280 (2004) 55–61.
[12] A.E. Ahmed, F. Adam, Microporous Mesoporous Mater. 103 (2007) 284–295.
[13] S. Ananda, A.B. Wiredu, Appl. Catal. A 417–418 (2012) 259–262.
[14] C. Breuil, J.N. Saddler, Enzyme Microb. Techol. 7 (1985) 327–332.
[15] G.L. Miller, Anal. Chem. 31 (1959) 426–428.
[16] F. Adam, H. Osman, K.M. Hello, J. Colloid Interface Sci. 331 (2009) 143–147.
[17] F. Adam, M.I. Saleh, I. Abd Al-Rahman, in: R. Othman (Ed.), Seramik Nusantara, Universiti Sains Malaysia, Penang, 1990, pp. 261–273.
[18] N. Yalcin, V. Sevinc, Ceram. Int. 27 (2000) 219–224.
[19] J.P. Nayak, J. Bera, Bull. Mater. Sci. 34 (2011) 1683–1687.
[20] M.C. Morris, H.F. McMurdie, E.H. Evans, B. Paretzkin, H.S. Parker, N.C. Panagiotopoulos, Standard X-ray Diffraction Powder Pattern, C 13.44: 25/sec. 18, Department of Commerce, U.S., 1981, pp. 24–25.
[21] M. Thommes, Chem. Ing. Tech. 82 (2010) 1059–1073.
[22] J.A. Melero, R. van Grieken, G. Morales, M. Paniagua, Energy Fuels 21 (2007) 1782–1791.
[23] M.D. González, P. Salagre, E. Taboada, J. Llorca, E. Molins, Y. Cesteros, Appl. Catal. B: Environ. 136–137 (2013) 287–293.
[24] Q. Yang, J. Liu, J. Yang, M.P. Kapoor, S. Inagaki, C. Li, J. Catal. 228 (2004) 265–272.
[25] A.R. Swoboda, G.W. Kunze, 13th national conference on clays and clay minerals (1964) 277–288.
[26] E. Modrogan, M.H. Valkenberg, W.F. Hoelderich, J. Catal. 261 (2009) 177–187.
[27] P.F. Siril, D.V. Davison, J.K. Randhawa, D.R. Brown, J. Mol. Catal. A: Chem. 267 (2007) 72–78.
[28] N. Bhatt, A. Patel, J. Taiwan Inst. Chem. Eng. 42 (2011) 356–362.
[29] F. Adam, M.S. Batagarawa, K.M. Hello, S.S. Al-Juaid, Chem. Pap. 66 (2012) 1048–1058.
[30] X. Wang, S. Cheng, C.C.J. Chan, C.H.J. Chao, Microporous Mesoporous Mater. 96 (2006) 321–330.
[31] R. Marschal, J. Rathousky, M. Wark, Chem. Mater. 19 (2007) 6401–6407.
[32] C. Li, J. Yang, X. Shi, J. Liu, Q. Yang, Microporous Mesoporous Mater. 98 (2007) 220–226.
[33] K.M. Hello, F. Adam, T.H. Ali, J. Taiwan Inst. Chem. Eng. (2013), http://dx.doi.org/10.1016/j.jtice.2013.04.018.
[34] Y. Liu, W. Xiao, S. Xia, P. Ma, Carbohydr. Polym. 92 (2013) 218–222.
[35] W. Su, MSc. Thesis, A study of cellulose dissolution in ionic liquid water brines, Umea University, Sweden, 2012, pp. 1–2.
[36] S. Dutta, S. De, M.I. Alam, M.M. Abu-Omar, B. Saha, J. Catal. 288 (2012) 8–15.
[37] C. L. McCormick, US Patent No. 4,278,790 (1981).
[38] A.F. Turbak, in: E.J. Soltes (Ed.), Wood and agricultural residues, Academic Press, New York, 1983, pp. 87–99.
[39] A.L. Dupont, Polymer 44 (2003) 4117–4126.